The Astrophysical Journal, 654:697–701, 2007 January 10

TIDAL DISRUPTION OF THE FIRST DARK MICROHALOS

HongSheng Zhao,[1,2] Dan Hooper,[3] Garry W. Angus,[1,2] James E. Taylor,[4] and Joseph Silk[5]

Received 2005 December 15; accepted 2006 August 30

ABSTRACT

We point out that the usual self-similarity in cold dark matter models is broken by encounters with individual normal galactic stars on a subparsec scale. Tidal heating and stripping must have redefined the density and velocity structures of the population of the Earth-mass dark matter halos, which are likely to have been the first bound structures to form in the universe. The disruption rate depends strongly on galaxy types and the orbital distribution of the microhalos; in the Milky Way, stochastic radial orbits are destroyed first by stars in the triaxial bulge, and microhalos on nonplanar retrograde orbits with large pericenters and/or apocenters survive the longest. The final microhalo distribution in the solar neighborhood is better described as a superposition of filamentary microstreams rather than as a set of discrete spherical clumps in an otherwise homogeneous medium. This has important consequences to our detections of microhalos by direct recoil signal and indirect annihilation signal.

Subject heading: dark matter

1. INTRODUCTION

The cold dark matter (CDM) model has had considerable success in accounting for the observed large-scale structure of our universe. On galactic and subgalactic scales, however, the abundance of low-mass structure and the degree of concentration of dark matter halos predicted by CDM simulations have provoked a considerable amount of discussion. To clarify how CDM behaves on the smallest scales, Diemand and collaborators recently performed the highest resolution numerical simulations of dark matter clustering to date (Diemand et al. 2005). These simulations start with an initial spectrum of density fluctuations extending down to the free-streaming mass of the dark matter candidate, which, for a generic weakly interacting 100 GeV particle (such as a supersymmetric neutralino), is roughly $\sim 10^{-6}(t_{\rm fo}/10^{-8}{\rm s})^{7/4}\,M_\odot$, where freezeout occurs at an epoch $t_{\rm fo} \sim 10^{-8}(m_\chi/100\ {\rm GeV})$ s. As expected from scaling the results of simulations on larger scales, fluctuations in this initial distribution collapse and virialize to form structures with roughly 200 times the background density at a redshift of $z \sim 50$. This first generation of "microhalos" survives to some degree as substructure in the larger halos that form subsequently in the simulations. Extrapolating to the present day, Diemand et al. (2005) suggest that 10^{15} Earth-mass clumps should survive in the halo of the Milky Way, amounting to about 0.1% of its total mass. If this were the case, the nearest Earth-mass clump would be on the order of 0.1 pc distant from the Earth and would have a typical size of 0.01 pc. Such nearby clumps might be observable as sources of gamma rays, which would be produced in dark matter annihilations. They might also contribute to diffuse cosmic-ray fluxes of positrons or antiprotons. In order to motivate experimental searches, however, it is important to determine whether the predicted small clumps of dark matter would actually survive the grainy tidal field due to stars while crossing the Galactic bulge and disk $\sim$100 times.

Here we estimate the rate at which Earth-mass clumps are disrupted in stellar encounters. We show that the nearest clumps in a galaxy like the Milky Way are likely to be tidally disrupted by repeated encounters over a Hubble time. Nevertheless, tidal debris from individual clumps may produce distinct microstreams that are potentially observable in dark matter detection experiments.

2. A SEMIANALYTICAL MASS-LOSS ESTIMATE

Extended bodies generally have a complex response to external tidal heating (Gnedin & Ostriker 1999). We can estimate the net effect of this process by applying the basic scaling from the semianalytical mass-loss model of Taylor & Babul (2001), which has been shown to match tidal heating and mass-loss rates in high-resolution numerical simulations. According to this model, whenever a system on a general orbit spends a time Δt in a strong tidal field—that is, a field in which the instantaneous tidal limit for the object $r_t(t)$ (calculated as in the circular-orbit case; see Binney & Tremaine 1987) is smaller than its size r—it loses a fraction $\Delta t/t_{\rm orb}$ of the mass outside $r_t(t)$, where $t_{\rm orb} = 2\pi r(t)/v(t)$ is the instantaneous orbital period.

To estimate when material at a radius r in a microhalo will experience strong shocks, we need to calculate the minimum impact parameter such that $r_t(t) < r$. This is equivalent to the condition that the tidal force generated during an encounter with a star of mass m_* at an impact parameter $b_{\rm sh}$, which is $2Gm_*x/b_{\rm sh}^3$, exceeds the restoration force for a small displacement x, which is $(4\pi G\rho_{<r}/3)x$, where $\rho_{<r}$ is the mean density of the microhalo interior to r. For a typical microhalo in the simulations by Diemand et al. (2005), the density at the half-mass radius is $\sim 1\ M_\odot\ {\rm pc}^{-3}$, while the highest resolved density (at $0.1r_{200}$) is $\sim$10 times higher. We do not expect a divergent (phase space) density in these smallest halos. Even if a cusp existed below the simulation resolution, it would contain less than 3% of the microhalo's mass, extrapolating from the profile given by Diemand et al. (2005). Thus, for a rapid encounter with a solar-mass star, impact parameters of $b_{\rm sh} \sim (m_*/\rho_{\rm mic})^{1/3} \sim 0.5$ pc or less will produce a strong shock over a range of radii containing 97% or more of the mass in the microhalo. The quantity $\rho_{\rm mic}$ is the average density within 10% of the virial radius $r_{\rm vir}$ and can be thought of as a constant until the microhalo is virtually destroyed, as shown in Angus & Zhao (2006, hereafter AZ06; see their Fig. 7*b*).

[1] National Astronomical Observatories, Chinese Academy of Sciences, Beijing, China.
[2] Scottish Universities Physics Alliance, School of Physics and Astronomy, University of St. Andrews, St. Andrews, UK.
[3] Fermi National Accelerator Laboratory, Batavia, IL.
[4] Department of Astronomy, California Institute of Technology, Pasadena, CA.
[5] Department of Astrophysics, University of Oxford, Oxford, UK.

A microhalo moving at a relative speed of $V_r \sim 300$ km s^{-1} through a star field with a number density $n_* = \rho_*/m_*$ will encounter stars with an impact parameter $\lesssim b_{\rm sh}$ at a rate of $\dot{N}_{\rm enc} = n_* V_r \pi b_{\rm sh}^2 \sim n_*/0.004$ pc^{-3} Myr^{-1}. Each encounter shocks the microhalo for a time $\Delta t = 2b/V_r \sim 3300$ yr and liberates a fraction of the microhalo's total mass. This fraction, from the scaling in Taylor & Babul (2001), is roughly $\Delta m/m = \Delta t/t_{\rm orb} = v_{\rm orb}/\pi V_r \sim 10^{-4}$. Here $t_{\rm orb} \equiv 2\pi b_{\rm sh}/v_{\rm orb} \sim 30$ Myr is the period of a circular orbit of speed $v_{\rm orb} = (Gm_*/b_{\rm sh})^{1/2} \sim 90$ m s^{-1} around the solar-mass perturber at a distance of $b_{\rm sh} \sim 0.5$ pc. Thus, the mass of a microhalo decreases exponentially, with the e-folding time given by $1/\tau \equiv -m^{-1}\, dm(t)/dt = \dot{N}_{\rm enc}\Delta m/m = Gn_* m_* (G\rho_{\rm mic})^{-1/2}$, where we have expressed b in terms of the parameters of the satellite. Averaged over a Hubble time, we find that a microhalo's mass decays exponentially, $m(t) = m_0 \exp(-t/\tau)$, where the e-folding time and the present mass are given by

$$\ln \frac{m_0}{m_{\rm now}} = \frac{10\ {\rm Gyr}}{\tau} \approx \frac{\langle \rho_* \rangle}{0.004\ M_\odot\ {\rm pc}^{-3}} \left(\frac{\rho_{\rm mic}}{10\ M_\odot\ {\rm pc}^{-3}} \right)^{-1/2}, \quad (1)$$

where $\langle \rho_* \rangle$ is the mass density of Galactic (disk, bulge, and halo) stars averaged along the orbit of a microhalo over the past 10 Gyr (at earlier times, few stars might have formed). In general, $\langle \rho_* \rangle$ is a function of the pericenter, apocenter, and vertical height of the microhalo orbit. For example, a microhalo on a thick-disk orbit of height 1000 pc near the solar neighborhood would have made $\sim$100 disk crossings and gone through star fields of an accumulated column density $\sim 10^4$ pc^{-2} by today. It goes through the Galactic disk with a mean surface density of 46 $M_\odot$ pc^{-2} or an average volume density of 46 $M_\odot$ pc^{-2}/2000 pc $\sim 0.023\, M_\odot$ pc^{-3}; thus, this microhalo's mass is predicted to have decayed by about 6 e-foldings.

Another way to think of the semianalytical disruption rate is to note that the logarithm of the bound fraction $\ln(m_{\rm now}/m_0) \propto \int \rho_*\, dt \propto \Sigma_*/V_r$, where Σ_* is the stellar mass density encountered. To get an indication of how robust the semianalytical mass-loss rate is, we have also run N-body simulations of a simplistic single encounter between a star and a microhalo for comparison. We use the tree code of Vine & Sigurdsson (1998), with a total particle number of 10^5 and a softening of 10^{-4} pc, consistent with interparticle separations of 3.5×10^{-4} pc. The tree code tolerance parameter, θ, is the cell size divided by the particle separation and is set to 0.6 in these simulations. Initially the microhalo particles were distributed in a spherical Navarro-Frenk-White (NFW) density profile with a value of $r_{\rm vir} = 1.6R_c = 0.01$ pc and a total mass of $10^{-6}\, M_\odot$. Two sets of velocity-space initial conditions were used: tangentially anisotropic (TA) microhalos with randomly inclined circular orbits $\overline{V_r^2}(r) = 0$, and radially anisotropic (RA) microhalos with $\overline{V_r^2}(r) = \overline{V^2}(r)/2 = \{1/[r\rho(r)]\} \int_r^{r_{\rm vir}} V_c^2 \rho\, dr$, where $\rho(r)$ and V_c are the microhalo's internal density and circular velocity, respectively (see AZ06). The two-body relaxation time, measured by the mean squared normalized energy drift after 10^4 time steps using 10^5 particles for an isolated microhalo, is about 3 Gyr. So a microhalo resolved with 10^5 particles should be free from numerical relaxation on timescales of 15 Myr; that is, the dynamical timescale of the microhalo. To measure the effect of encounters with stars, we shoot a single star of mass $M_* = 0.1$, 0.3, 0.6, and 1 $M_\odot$ with a relative velocity of $V_r = 200$ km s^{-1} toward a microhalo with a closest approach $b = (0.2\text{–}1)r_{\rm vir}$ for penetrative encounters and $(1\text{–}4)r_{\rm vir}$ for nonpenetrative encounters. Such an impact is typical for a microhalo passing through a random star field with an equivalent star column density $\Sigma_* = M_*/(\pi b^2)$. The duration of a star passage, say, along the x-axis from $x = 10r_{\rm vir}$ to $-10r_{\rm vir}$ is about 0.0001 dynamical times of the microhalo; hence, microhalo particles are virtually stationary (moving less than 0.01% of the orbital radius) during a star passage, so the perturbations are indeed in the impulse regime. It appears that our semianalytical model captures the essential feature in numerical simulations of the impulse on $10^{-6}\, M_\odot$ microhalos, if we assume $\rho_{\rm mic} \sim 1\, M_\odot$ pc^{-3} (see Fig. 1). However, there are microhalos of a few times Earth mass, and these can be, for example, 5 times more massive and denser than the $10^{-6}\, M_\odot$ microhalos experimented with here (see Fig. 2 of Diemand et al. 2005). Allowing for more robust microhalos, and to be conservative in estimating the disruption rate of microhalos, we adopt the rate from the semianalytical model, assuming $\rho_{\rm mic} \sim 10\, M_\odot$ pc^{-3} hereafter. Note that the scaling of our semianalytical model, equation (1), also agrees with the literature on impulse-induced mass loss in the context of diffuse star clusters, such as Moore (1996) and equations (6)–(8) of Wielen (1985) or equation (8) of Wasserman & Salpeter (1994).

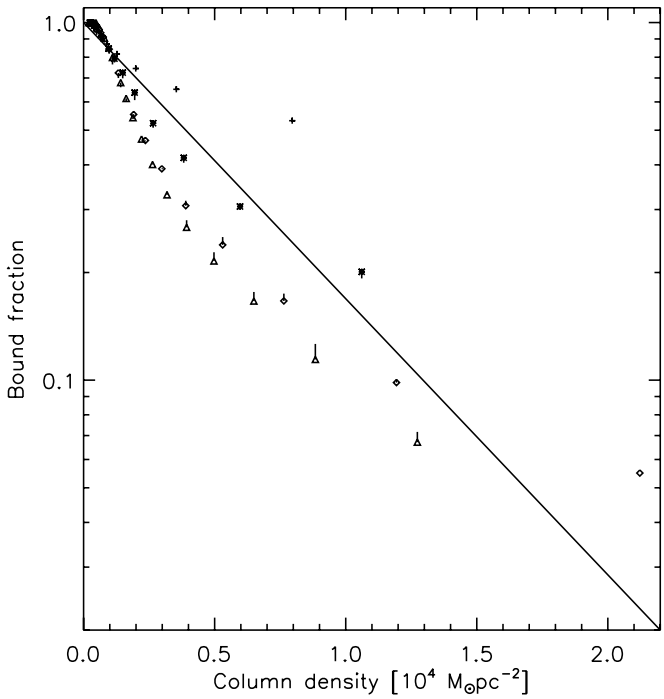

FIG. 1.—Postimpulse fraction of bound microhalo particles vs. the equivalent column density $\Sigma_* = M_*/(\pi b^2)$ of the perturbers, where symbols and vertical lines denote results from a set of numerical experiments of stellar encounters with microhalos of initially tangential anisotropy (TA) and radial anisotropy (RA). The symbols indicate the RA microhalos, and the vertical lines end at the position of the TA microhalos. In these experiments a perturber with $M_* = 0.1\, M_\odot$ (*plus signs*), 0.3 $M_\odot$ (*asterisks*), 0.6 $M_\odot$ (*diamonds*), or 1 $M_\odot$ (*triangles*) passes a $10^{-6}\, M_\odot$ microhalo with relative velocity $V_r = 200$ km s^{-1} and different values of the impact parameter b, ranging from penetrative ($b < r_{\rm vir}$) to nonpenetrative encounters ($b > r_{\rm vir}$). For the same mass column density, many low-mass penetrative perturbers are not as efficient as a few high-mass nonpenetrative perturbers in terms of stripping the microhalo; stripping is unimportant for substellar perturbers in general. Our semianalytical prediction assuming $\rho_{\rm mic} = 10\, M_\odot$ pc^{-3} is represented by the solid line.

3. MICROHALOS ON NEAR-EARTH ORBITS

To study the dependence of mass loss on orbital parameters, we have integrated orbits of microhalos in a flattened, axisymmetric galaxy potential with a nearly flat rotation curve: $\Phi(R, z) = (220\ {\rm km\ s^{-1}})^2 \ln\{(R^2 + z^2/0.8)^{1/2}[(R^2 + z^2)^{1/2} + 60\ {\rm kpc}]^{-1}\}$.

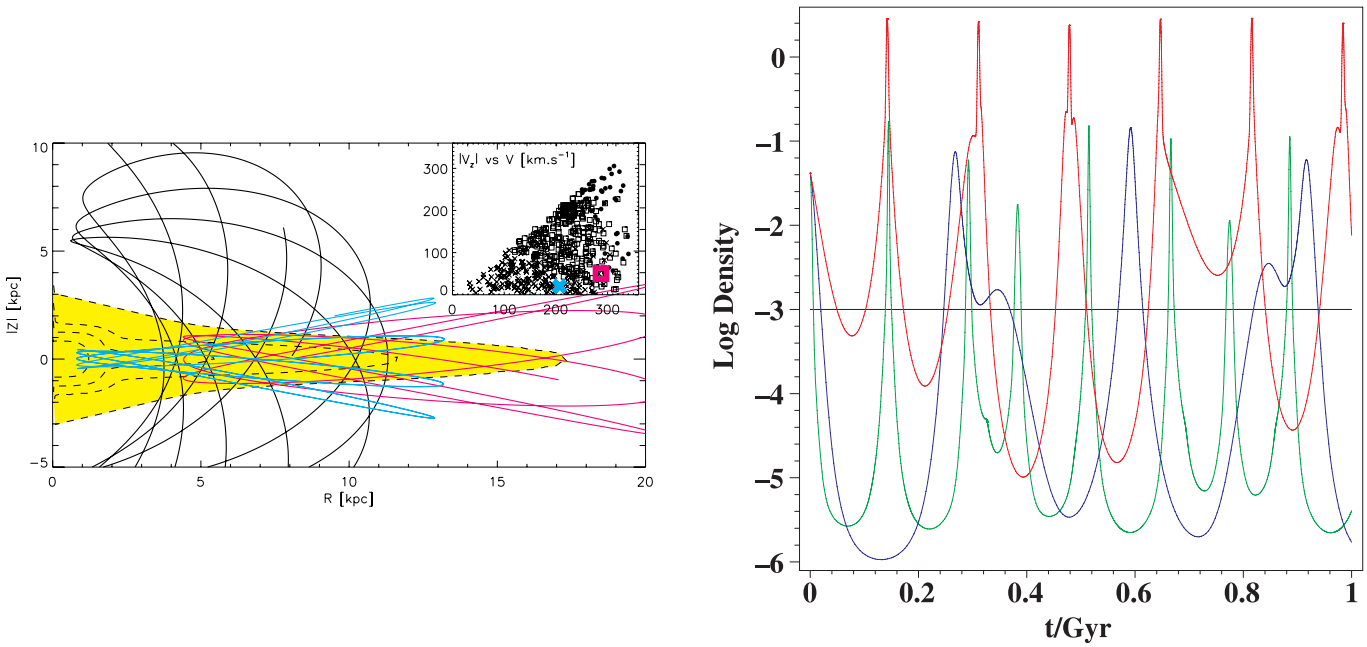

FIG. 2.—Variations of star density for different orbits in the Galaxy. *Left*: The inset shows the scatter diagram of the velocity space (at launch) for the 500 microhalos launched from the solar circle. Microhalos are given different symbols depending on the time-averaged stellar density along the orbits ($\langle\rho_*\rangle > 0.01\ M_\odot\ \mathrm{pc}^{-3}$, *crosses*; $<0.001\ M_\odot\ \mathrm{pc}^{-3}$, *filled circles*; in between, *squares*). Note that microhalos with low orbital energy and angular momentum are the first to be disrupted. Three typical orbits (*larger symbols*) are picked out and shown in the meridional plane Z vs. R in the left panel. The yellow shaded area is a cut of the Besançon star count model of the Galaxy (Robin et al. 2003) with an equal star density of $10^{-i}\ M_\odot\ \mathrm{pc}^{-3}$ for $i = 0$, 1, 2, and 3, plotted in contours. *Right*: Star density, in units of $M_\odot\ \mathrm{pc}^{-3}$, along the three orbits as a function of time. The cyan orbit in the left panel corresponds to the red curve in the right panel, the black orbit corresponds to the green curve, and the magenta orbit corresponds to the blue curve.

We launch 500 orbits from the solar neighborhood, $(R, z) = (8\ \mathrm{kpc}, 0)$, with a Gaussian velocity distribution (150 km s^{-1} dispersion in each direction). We read off the stellar density along the orbit using the Besançon model of the Galaxy (Robin et al. 2003) and then take a time average of the star density. The Besançon model is a widely accepted detailed prescription of the number density of stars and stellar remnants of different ages and masses in the Galactic spheroids (bulge and halo) and disks (thin and thick). A few examples of the microhalo orbits are given together with the star count model in the left panel of Figure 2. These simulations suggest that the population of microhalos with apocenters less than 12 kpc has $\langle\rho_*\rangle \sim 0.002\ M_\odot\ \mathrm{pc}^{-3}$ and that the microhalos are hence past their half-life (Fig. 2, *black orbit*). The more planar orbits, with $|Z| \lesssim 4(R/20)$ kpc and apocenter $R \lesssim 20$ kpc (Fig. 2, *magenta orbit*), have decayed by approximately 1 *e*-folding time with $\langle\rho_*\rangle \sim 0.004\ M_\odot\ \mathrm{pc}^{-3}$. Complete destruction should happen to disky orbits penetrating into the bulge; for example, the cyan orbit in Figure 2 goes through a typical column density of 500 $M_\odot\ \mathrm{pc}^{-2}$ with each disk crossing at a small angle, and has on average $\langle\rho_*\rangle \gtrsim 0.075\ M_\odot\ \mathrm{pc}^{-3}$, corresponding to about 19 *e*-folding times. In general, we observe a strong correlation between the orbital shape and the disruption rate. Orbits that go through dense regions of the Galaxy are likely disrupted due to tides (see Fig. 2).

Also plotted in the inset of Figure 2 is the zone of destruction in the velocity space using 500 microhalos launched from the solar neighborhood. There is a clear trend for halos with more planar (smaller $|V_z|$) orbits, especially those corotating with the disk, and orbits with lower energy (and hence smaller apocenters) to enter regions of higher density. The sample average density is 0.008 $M_\odot\ \mathrm{pc}^{-3}$ or 0.02 $M_\odot\ \mathrm{pc}^{-3}$ for median or mean density, so microhalos on Earth-crossing orbits are likely to have been severely stripped. About 10% of the microhalos are in low-density regions (below 0.001 $M_\odot\ \mathrm{pc}^{-3}$) and might survive more or less intact. The chance of survival, however, is likely even more severely reduced in the triaxial, barred, and evolving potential of the Milky Way, where most orbits are stochastic box orbits that pass through the dense center of the Milky Way at some point over a Hubble time. In addition, it has been shown in AZ06 that disk shocking and tidal stripping may combine with stellar encounters to destroy microhalos even more efficiently than shown here.

Of course, these orbits are merely a sample of all orbits passing the Sun. In fact, the fraction of halos disrupted would be much lower for high-energy orbits beyond the solar neighborhood as the tides at larger pericenter are weaker along with the rapidly decreasing fraction of stars. What was also keenly noted by Berezinsky et al. (2006) was that apocentric disk crossings beyond the extent of the thin disk are likely to boost the lifetime of microhalos. The destruction rate is certainly much higher for low-energy orbits contained inside the bulge or those that have pericenters within the solar radius. These microhalos would be exposed to stronger tides and higher stellar densities, added to the fact that they will cross the disk twice every orbit. However, these orbits are irrelevant for direct experiments on Earth and are less important for indirect experiments because microhalos are barely identifiable from the background beyond about a distance of 0.1–1 pc from us.

In addition, the calculations done by Diemand et al. (2005) did not find self-consistent orbits, and their comments on the current situation in the Milky Way are major extrapolations from dark matter–only simulations that stop at redshift 26 and only ever simulate a much smaller total volume. Since halo orbits would be strongly affected by the formation of the Milky way, the disruption rate is a function of orbital parameters.

We note that the long-term fate of the cusp at the very center of each microhalo is unclear. Simulations have shown that systems

with a universal density profile may lose all but 0.1%–1% of their mass and still retain a bound central region (Hayashi et al. 2003). Such objects may indeed survive to the present day in the solar neighborhood, but they will have little effect on dark matter detection experiments. The tidal debris stripped out of microhalos may actually be of greater interest, as discussed below. Nevertheless, AZ06 (see their Fig. 7*b*) showed that the inner density of a microhalo ($\rho_{\rm mic}$) is largely unaffected until it is stripped down to the inner shell.

4. IMPLICATIONS FOR DIRECT AND INDIRECT DETECTION

The existence of dark substructure in our Galaxy's halo has important implications for the prospects of both direct and indirect dark matter detection (Green et al. 2005; Berezinsky et al. 2003; Pieri et al. 2005; Koushiappas et al. 2004). The presence of substructure affects direct detection rates in a straightforward way: If the solar system happens to be located inside an overdense region of dark matter, then the rate observed will be enhanced proportionally to the density of the clump. If, as is much more likely, our solar system is not inside a clump, then the rate will be modestly reduced by the fact that some fraction of the overall density is contained in substructures and thus does not contribute to the density of the smooth component.

Zhao & Silk (2005) estimated that the nearest minihalo of $10^6\,M_\odot$ is 1 kpc away with a size of 50 pc. Diemand et al. (2005) estimated that unstripped Earth-mass halos have a filling factor of 0.5%. Hence, in either case it is *unlikely* for the Sun to be inside a substructure.

Tidal debris from encounters with stars changes the picture substantially. While the probability to find our solar system inside a 10^{-4} pc–sized bound remnant of a microhalo is on the order of 10^{-8}, the probability is of order unity for the solar system to be moving presently inside an (unbound) substructure. Disrupted streams are inhomogeneous regions with at least 10 times the volume filling factor of the original unstripped clump. This is because at each disk crossing a burst of tidal debris is released due to encounters with disk stars, and the tails would lead/trail at least 0.1 pc (assuming a 1 m s^{-1} speed of escape) along the system's trajectory in 100 Myr, the time between disk crossings. The time for the solar system to cross a stream at a general angle will be longer than 50 yr, the time to cross a bound microhalo (Diemand et al. 2005). Moving inside the inhomogeneous debris of the microhalos could cause transient enhancements of the event rate in direct detection experiments. Furthermore, clumps on polar orbits survive longer than planar orbits (see Fig. 2); this makes the velocity distribution of the microstreams non-Gaussian and could imprint an interesting annual modulation on the direct detection signal (Morgan et al. 2005; Freese et al. 2005). Figure 12 of AZ06 shows the morphology of a microstream: even after the microhalo is fully disrupted, the microstream is still a distinct entity with a negligible tangential size compared to its length. As a result, these filamentary streams may be the fate of a large proportion of the Milky Way's microhalos, and the enhanced background from these structures may impose interesting features on direct detection experiments, as well as having interesting annihilation flux properties.

The implications of dark microhalos and microstreams are rather different for the case of indirect detection. Indirect measurements sample the distribution of dark matter, through its annihilation rate, over large regions of the halo. Furthermore, dark matter annihilation rates, and thus indirect detection signals, are proportional not to the density of dark matter, but to the dark matter density squared. Substructure within the Galactic halo thus may be capable of boosting the dark matter annihilation rate and enhancing the prospects of detecting dark matter indirectly (Taylor & Silk 2003).

Techniques employed for the indirect detection of dark matter include gamma-ray, antimatter, and neutrino detectors (Silk & Srednicki 1984). Gamma rays annihilating in nearby and dense substructures, if present, could provide point sources potentially observable by gamma-ray telescopes (Pieri et al. 2005; Koushiappas et al. 2004). Antimatter produced in dark matter annihilations is deflected by Galactic magnetic fields, and thus only the diffuse spectrum can be studied. Neutrinos are not as useful for identifying annihilations in the Galactic halo, but instead are used to search for dark matter particles annihilating in the core of the Sun. The neutrino flux produced through dark matter annihilations in the Sun is tied to the local density averaged over very long periods of time, and therefore the presence of substructure is of little importance.

Nearby microhalos, being tidally disrupted, are not particularly bright point sources of gamma rays. While Diemand et al. (2005) predict that the nearest intact microhalo will be much brighter than known dwarf spheroidals in gamma rays, we find that the situation is reversed for a microhalo left with only a 1% bound remnant.

Antimatter fluxes produced through dark matter annihilations do not depend on the nature or location of individual dark substructures, but rather on the distribution of dark matter averaged over large volumes. The value of the quantity $\langle\rho^2\rangle/\langle\rho\rangle^2$, averaged over the contributing volume (a few kpc for positrons or tens of kpc for antiprotons), determines the overall boost factor for the antimatter fluxes generated through dark matter annihilations.

With a distribution of substructure of the form $dN/d\log M \propto M^{-1}$, each decade of mass contributes almost equally to the boost factor, so it is important to determine over what range of masses substructures can survive. Previous works (Helmi et al. 2002; Stoehr et al. 2003) emphasized the role of larger substructures, with the mass of the Draco dwarf spheroidal. Diemand et al. (2005) argue that the nearest Earth-mass halo is a factor of a few brighter than Draco. We argue, however, that the nearest Earth-mass halo is likely to be tidally dispersed and hence fainter than Draco. We have proposed (Zhao & Silk 2005) that the nurseries of the first stars in the universe were dense minihalos of $10^6\,M_\odot$ formed at $z \sim 22$. Unlike the microhalos, such minihalos can survive the Galactic tides until the present day. The nearest minihalo is only 1–2 kpc from the Sun and is an order of magnitude brighter than the combined annihilation from the Draco galaxy.

In light of the excess reported by the High-Energy Antimatter Telescope (HEAT) collaboration (Barwick et al. 1997; Coutu et al. 1999; Baltz & Edsjö 1999), substructure is of particular importance for dark matter searches involving positrons. To produce such a signal with thermally generated neutralinos or other type of weakly interacting massive particles (WIMPs), however, boost factors of $\sim$50 or higher are required (Baltz et al. 2005; Hooper & Kribs 2004; Hooper & Servant 2005). Although it has been shown that more massive substructures do not naturally provide such a large boost factor (Hooper et al. 2004; Hooper & Silk 2005), effects due to baryons or the presence of intermediate-mass black holes could perhaps make them brighter (Prada et al. 2004), although probably not enough to account for the HEAT excess. After the effects of tidal disruption are considered, the same is found to be true for Earth-mass microhalos. We agree with previous studies (Berezinsky et al. 2003) that determine that positron boost factors larger than $\sim$2–5 are unlikely. Given this conclusion, another explanation for the excess observed by HEAT

appears to be required. Our understanding of these issues will be dramatically improved with data from the upcoming cosmic antimatter experiments PAMELA and AMS-02 (Profumo & Ullio 2004).

5. DISCUSSION AND CONCLUSIONS

Using a semianalytical estimate of the tidal mass-loss rate, together with numerical integration of a fair sample of microhalo orbits, we find that most microhalos present in the solar neighborhood will have been heavily stripped by stellar encounters, producing "microstreams" of tidal debris. More generally, in environments with very low stellar densities, such as the outer parts of the Galactic disk or in a Sextans-like dwarf galaxy, microhalos are only mildly heated. But in high-density environments such as the Galactic bulge or an M32-like elliptical galaxy (800–0.05 $M_\odot$ pc^{-3} in the inner 1 kpc of M32; Mateo 1998), microhalos are likely fully destroyed. In disk galaxies such as the Milky Way, the fraction of microhalos that are disrupted depends strongly on the orbital inclination and pericenter. Microhalos on orbits coplanar with the disk are very quickly disrupted. Microhalos in the outer part of galaxy halos will encounter far fewer stars, however, and thus their annihilation rates will be less dramatically reduced. A possible consequence of this might be to detect little gamma-ray emission from the central part of external galaxies, where stars have disrupted most of the dark substructure, and more flux from the outer regions. A ring of gamma rays surrounding a galaxy, if detected, would provide a strong confirmation of the existence of dark substructure.

The tidal effects discussed in this paper have important consequences for the direct and indirect detection of dark matter. In particular, the probability of the Earth intersecting a tidal stream at any given time is considerably larger than the probability of it being inside a microhalo's bound remnant, and thus tidal streams may potentially increase the reach of direct detection experiments. Indirect detection rates are not enhanced, however, as once stellar encounters are considered, Earth-mass halos are not a significant contributor to the overall dark matter annihilation rate.

H. Z. acknowledges support from PPARC Advanced Fellowship and Outstanding Oversea Young Scholarship from the Chinese Academy of Science. G. W. A. acknowledges an overseas fieldwork grant from PPARC and hospitality from Beijing University. J. E. T. acknowledges financial support from the NSF (grant AST 03-07859) and the DoE (contract DE-FG02-04ER41316).

REFERENCES

Angus, G. W., & Zhao, H. 2006, MNRAS, submitted (AZ06)
Baltz, E. A., & Edsjö, J. 1999, Phys. Rev. D, 59, 023511
Baltz, E. A., Edsjö, J., Freese, K., & Gondolo, P. 2003, in Proc. 4th Int. Workshop on Identification of Dark Matter, ed. N. J. C. Spooner & V. Kudryavtsev (Singapore: World Scientific), 489
Barwick, S. W., et al. 1997, ApJ, 482, L191
Berezinsky, V., Dokuchaev, V., & Eroshenko, Y. 2003, Phys. Rev. D, 68, 103003
———. 2006, Phys. Rev. D, 73, 063504
Binney, J. J., & Tremaine, S. 1987, Galactic Dynamics (Princeton: Princeton Univ. Press)
Coutu, S., et al. 1999, Astropart. Phys., 11, 429
Diemand, J., Moore, B., & Stadel, J. 2005, Nature, 433, 389
Freese, K., Gondolo, P., & Newberg, H. J. 2005, Phys. Rev. D, 71, 043516
Gnedin, O. Y., & Ostriker, J. P. 1999, ApJ, 513, 626
Green, A. M., Hofmann, S., & Schwarz, D. J. 2005, J. Cosmol. Astropart. Phys., 8, 3
Hayashi, E., Navarro, J. F., Taylor, J. E., Stadel, J., & Quinn, T. M. 2003, ApJ, 584, 541
Helmi, A., White, S. D., & Springel, V. 2002, Phys. Rev. D, 66, 063502
Hooper, D., & Kribs, G. D. 2004, Phys. Rev. D, 70, 115004
Hooper, D., & Servant, G. 2005, Astropart. Phys., 24, 231
Hooper, D., & Silk, J. 2005, Phys. Rev. D, 71, 083503
Hooper, D., Taylor, J. E., & Silk, J. 2004, Phys. Rev. D, 69, 103509
Koushiappas, S. M., Zentner, A. R., & Walker, T. P. 2004, Phys. Rev. D, 69, 043501
Mateo, M. 1998, ARA&A, 36, 435
Moore, B. 1996, ApJ, 461, L13
Morgan, B., Green, A. M., & Spooner, N. J. 2005, Phys. Rev. D, 71, 103507
Pieri, L., Branchini, E., & Hofmann, S. 2005, Phys. Rev. Lett., 95, 211301
Prada, F., Klypin, A., Flix, J., Martínez, M., & Simonneau, E. 2004, Phys. Rev. Lett., 93, 241301
Profumo, S., & Ullio, P. 2004, J. Cosmol. Astropart. Phys., 7, 6
Robin, A. C., Reylé, C., Derrieré, S., & Picaud, S. 2003, A&A, 409, 523
Silk, J., & Srednicki, M. 1984, Phys. Rev. Lett., 53, 624
Stoehr, F., White, S. D., Springel, V., Tormen, G., & Yoshida, N. 2003, MNRAS, 345, 1313
Taylor, J. E., & Babul, A. 2001, ApJ, 559, 716
Taylor, J. E., & Silk, J. 2003, MNRAS, 339, 505
Vine, S., & Sigurdsson, S. 1998, MNRAS, 295, 475
Wasserman, I., & Salpeter, E. 1994, ApJ, 433, 670
Wielen, R. 1985, in IAU Symp. 113, Dynamics of Star Clusters, ed. J. Goodman & P. Hut (Dordrecht: Reidel), 449
Zhao, H., & Silk, J. 2005, Phys. Rev. Lett., 95, 011301